

Université de Mons

**Faculté Polytechnique – Service de Mécanique Rationnelle, Dynamique et Vibrations**

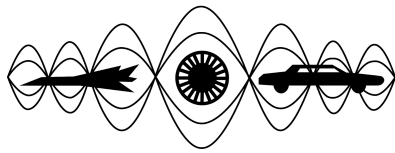
31, Bld Dolez - B-7000 MONS (Belgique)

065/37 42 15 – georges.kouroussis@umons.ac.be

---



G. Kouroussis, X. Siebert, B. Olivier, Using neural networks to calibrate a lumped mass model for track–soil vibration coupling, *Proceedings of the 31th International Congress on Sound and Vibration*, Incheon (Korea), July 6–11, 2025.



# USING NEURAL NETWORKS TO CALIBRATE A LUMPED MASS MODEL FOR TRACK-SOIL VIBRATION COUPLING

Georges Kouroussis<sup>1</sup>, Xavier Siebert<sup>2</sup> and Bryan Olivier<sup>1</sup>

*1 Université de Mons – UMONS, Faculty of Engineering, Department of Theoretical Mechanics, Dynamics and Vibrations, Place du Parc, 20 — 7000 Mons (BELGIUM)*

*e-mail: georges.kouroussis@umons.ac.be*

*2 Université de Mons – UMONS, Faculty of Engineering, Department of Mathematics and Operational Research, Place du Parc, 20 — 7000 Mons (BELGIUM)*

This paper addresses the problem of railway vibrations induced by moving trains and their modelling. An important aspect of this modelling is, undoubtedly, the track-soil interaction, which plays a significant role in generating seismic waves and enables an accurate description of low-frequency vibrations. In the past, a coupled lumped mass (CLM) model for the soil was developed, based on calibration with an equivalent finite element model that simulates the corresponding soil behaviour. While this approach allows for the use of a simplified track-soil model, it requires excessive computational resources during the calibration process. The aim of this research is to establish a straightforward link between the CLM model parameters (masses, stiffness, and damping coefficients) and common soil dynamic characteristics. To achieve this, a neural network is employed to establish this relationship. The neural network's training and testing database is generated using finite element simulations. The results show that the neural network can determine the CLM model parameters with sufficient accuracy, reproducing the same dynamic behaviour of the soil.

*Keywords: neural network, CLM model, railway, finite element methods*

---

## 1. Introduction

Contrary to vehicle-road interaction issues, the dynamic train-track-soil interaction represents a fully coupled problem, requiring the simultaneous solution of the equations of motion for the train, track, and soil [1, 2]. Regarding track-soil coupling, the Winkler foundation is entirely sufficient for modelling continuous subgrade. However, when discrete support (aka sleepers) is used, a single distributed foundation fails to predict the expected interaction accurately [3].

Rücker [4] investigated the interaction between sleepers and the soil in the context of high-speed vehicles to define a coupling condition. This condition was later revised and redefined by Knothe and Wu [5]. Knothe and Wu demonstrated that track-soil coupling primarily influences the low- and mid-frequency ranges, contradicting Rücker's initial assumption that it is significant at low vehicle speeds. Furthermore, they advised against using the Winkler foundation model to represent the ground's distributed stiffness and damping, as it does not account for the coupling between sleepers through the soil.

Their findings highlighted the critical role of sleeper coupling and demonstrated the individual contribution of each sleeper's contact with the soil.

The Winkler and generalized Winkler models are widely used in geotechnical engineering, particularly for analysing the dynamic impedance of foundations. Gazetas [6] emphasized the practical utility of single-degree-of-freedom systems in addressing soil–foundation interaction challenges. Least-squares calibration methods provide a historical approach to calculating equivalent foundation mass, damping, and stiffness matrices [7].

To avoid complex and huge models, including for example co-simulation techniques [8, 9], it is proposed in this paper to focus on discrete models, such as those found in various predictive approaches for vibrations induced by railway traffic (for example [10–13]), and using machine learning techniques to optimize the parameter definition process. An existing model, called CLM model, is used with a new approach to characterize the parameters that define them, leveraging machine learning techniques for optimization.

## 2. CLM model

### 2.1 Modelling approach overview

The mechanical track/soil model recently proposed by Kouroussis et al. [14] is briefly discussed in this paper. The flexible rail is characterized by its Young's modulus ( $E_r$ ), geometrical moment of inertia ( $I_r$ ), cross-sectional area ( $A_r$ ), and density ( $\rho_r$ ). Viscoelastic properties of the railpads and ballast are modelled using springs and dampers, with stiffness and damping parameters ( $k_p$  and  $d_p$  for the railpads,  $k_b$  and  $d_b$  for the ballast).

The CLM model for the foundation builds upon an extension of Lysmer's analogue foundation. In addition to the foundation's mass ( $m_f$ ), stiffness ( $k_f$ ), and damping ( $d_f$ ), supplementary spring-dashpot systems with stiffness ( $k_c$ ) and damping ( $d_c$ ) are incorporated to represent the coupling between sleeper–foundation contact areas. Reduced expressions for transmissibility have been developed to determine these five parameters for various soil types, whether homogeneous or layered. Notably, the damping parameter  $d_c$  can take negative values to account for ground wave propagation delay [14].

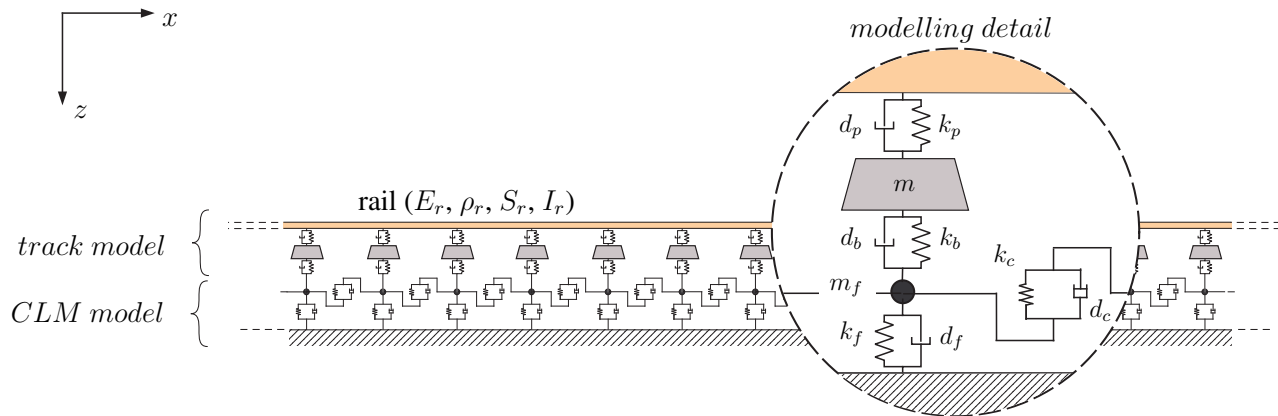


**Figure 1.** The flexible track, taking into account a condensed soil (represented by the CLM model) [15]

The validation has been made for both homogeneous and layered half-space [14, 15]. The methodology has been developed and adapted to ballasted track but it can be transposed to underground network: the track model with the condensed form of foundation can be used, as the foundation parameters can be estimated by updating numerical soil response receptances.

As totally performed in the time domain, this approach can be easily included in the vehicle design process, with more accurate and advanced models of track. The limitation initially induced by the decoupling can be also lifted with a more detailed model than the Winkler foundation.

## 2.2 Calibration

The proposed model is schematically illustrated in Figure 2 and consists of discrete masses, springs, and dampers.

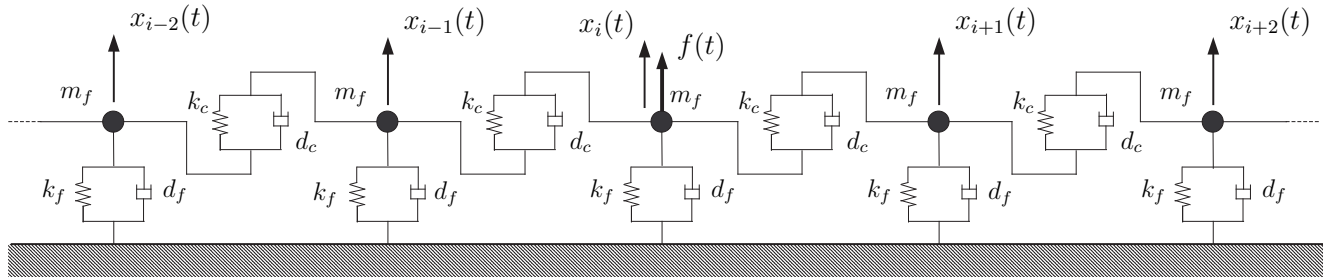


**Figure 2.** The CLM model: a multi-foundation model for soil–foundation and foundation–to–foundation interaction [14]

Based on the initial Lysmer's analogue model for each foundation (i.e., the sleeper-through-the-ballast contact area defined with a mass  $m_f$ , a spring  $k_f$  and a damper  $d_f$ ), each foundation is connected to the adjacent ones by springs (with parameter  $k_c$ ) and dampers (with parameter  $d_c$ ). Considering that a force is applied to the  $i$ -th mass, the overall impedances  $P_1$  and  $P_2$  for each vertical displacement  $x_j$  are [14]

$$P_1(\omega) = \frac{F(\omega)}{\sum_{j=-n}^n X_j(\omega)} = k_f - \omega^2 m_f + j\omega d_f \quad (1)$$

$$P_2(\omega) = \frac{F(\omega)}{\sum_{j=-n}^n (-1)^j X_j(\omega)} = (k_f + 4k_c) - \omega^2 m_f + j\omega(d_f + 4d_c) \quad (2)$$

where  $F(\omega)$  and  $X_j(\omega)$  are the Fourier transforms of force  $f(t)$  and displacements  $x_j(t)$  respectively, as a function of the circular frequency  $\omega$ . Eqs. (1) and (2) give unique relationships to calibrate CLM model parameters. Those parameters can be easily calculated using a finite element model of the soil, by applying a known force at a given point (mass) and recording the vertical displacement spectrum at  $n$  points (sufficiently high to capture the entire ground wave propagation).

For each soil type considered, a finite element numerical simulation is performed, for instance, using ABAQUS (Figure 3). To prevent spurious wave reflections, specific boundary conditions are imposed using infinite elements. The dynamic simulation yields the vertical displacement at  $n$  points on the soil surface. The displacement histories of these points are then applied in Eqs. (1) and (2) to manually calibrate the parameters of the CLM model corresponding to the soil. This calibration process is tedious, as it requires conducting a numerical simulation for each specific soil configuration. These simulations are computationally demanding, with the finite/infinite element models requiring several hours due to the high number of elements involved. Furthermore, the calibration process involves manual adjustments, where parameters  $P_1$  and  $P_2$  are tuned to minimize local discrepancies in the real and imaginary spectra between the CLM and ABAQUS models.

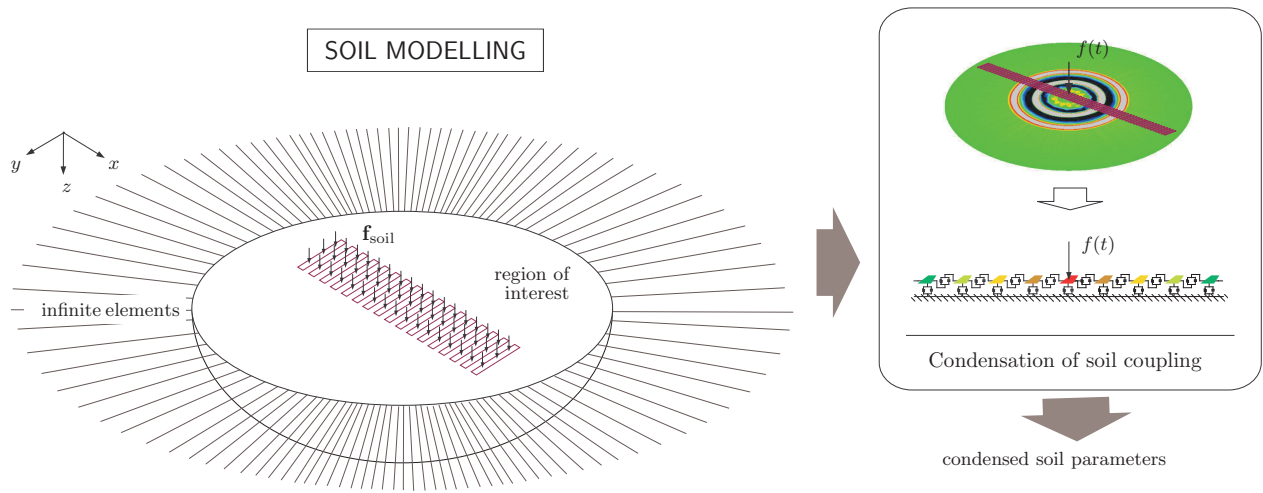


**Figure 3.** The finite/infinite element model for the soil, used for calibrating the CLM model

### 3. On the use of neural networks

Artificial neural networks are popular machine learning techniques that offer new insights in fitting operations, compared to standard techniques such as numerical optimization or statistical methods [16]. Training a neural network to approximate the relationship between inputs and outputs is particularly effective for complex, non-linear problems, if enough training data are available.

For the current issue, the structure of the five artificial neural networks designed to calculate the parameters of the CLM model can be described as follows:

1. **Number of Networks:** Five separate neural networks are implemented, each dedicated to predicting one of the CLM model parameters ( $k_f$ ,  $d_f$ ,  $m_f$ ,  $k_c$ , and  $d_c$ ).
2. **Input Layer:** Each network takes normalized soil characteristics (Young modulus  $E$ , density  $\rho$ , Poisson ratio  $\nu$ , viscous damping coefficient  $\beta$ ) as input, typically represented by four neurons.
3. **Hidden Layers:** The number of hidden layers and neurons per layer may vary depending on the complexity required. For instance, each network has one hidden layer with 10 to 20 neurons, using activation functions such as the sigmoid function.
4. **Output Layer:** Each network has a single output neuron, which provides the corresponding normalized CLM model parameter ( $k_f$ ,  $d_f$ ,  $m_f$ ,  $k_c$ , or  $d_c$ ).
5. **Training:**
  - The networks are trained using back propagation with a suitable optimizer and a loss function like mean squared error to minimize prediction error.
  - The training data is derived from one hundred numerical simulation results, ensuring sufficient variation in soil properties for generalization.
6. **Normalization and denormalization:** Both input and output data are normalized to facilitate training. To improve network convergence during training, the inputs to the neural networks are normalized between 0 and 1. While this normalization is not mandatory, it helps ensure that the synaptic weight values remain within the same order of magnitude. The output values are later denormalized to retrieve the actual CLM model parameters.

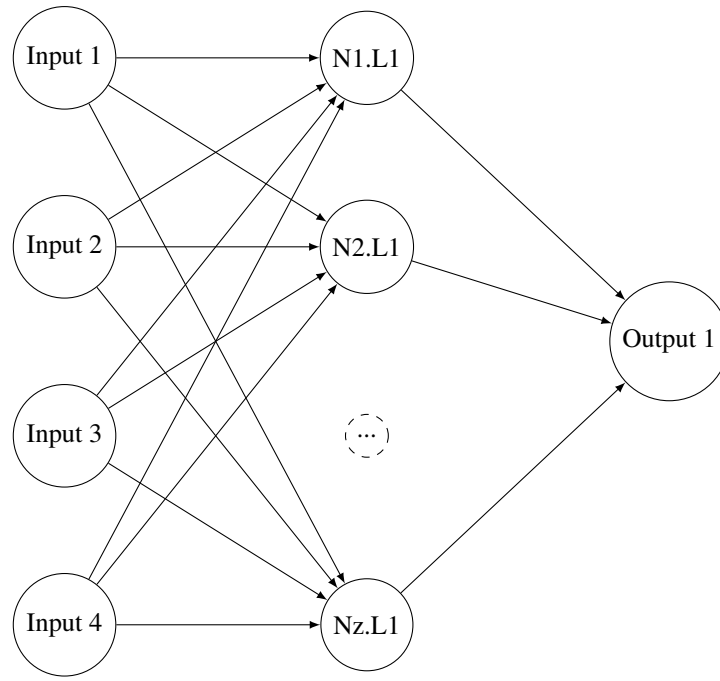


**Figure 4.** Structure of the five artificial neural networks to calculate the parameters of the CLM model

The input values for the neural networks are obtained by normalizing the soil characteristics using a chosen maximum value as follows:

- input representing  $E$  :  $E/400$  [MPa],
- input representing  $\rho$  :  $\rho/2600$  [kg/m<sup>3</sup>],
- input representing  $\nu$  :  $\nu/0.45$  [–],
- input representing  $\beta$  :  $\beta/0.0013$  [s].

When the neural networks have been trained, it becomes possible to predict the parameters of the CLM model for a given soil. This is calculated using the following matrix relations:

$$k_f = 120 \operatorname{sigm} \left( \operatorname{sigm} \left( \begin{bmatrix} \frac{E}{400} & \frac{\rho}{2600} & \frac{\nu}{0.45} & \frac{\beta}{0.0013} \end{bmatrix} \cdot \mathbf{W}_{1kf} \right) \cdot \mathbf{W}_{2kf} \right) \quad (3)$$

$$d_f = 350 \operatorname{sigm} \left( \operatorname{sigm} \left( \begin{bmatrix} \frac{E}{400} & \frac{\rho}{2600} & \frac{\nu}{0.45} & \frac{\beta}{0.0013} \end{bmatrix} \cdot \mathbf{W}_{1df} \right) \cdot \mathbf{W}_{2df} \right) \quad (4)$$

$$k_c = 60 \operatorname{sigm} \left( \operatorname{sigm} \left( \begin{bmatrix} \frac{E}{400} & \frac{\rho}{2600} & \frac{\nu}{0.45} & \frac{\beta}{0.0013} \end{bmatrix} \cdot \mathbf{W}_{1kc} \right) \cdot \mathbf{W}_{2kc} \right) \quad (5)$$

$$m_f = 260 \operatorname{sigm} \left( \operatorname{sigm} \left( \begin{bmatrix} \frac{E}{400} & \frac{\rho}{2600} & \frac{\nu}{0.45} & \frac{\beta}{0.0013} \end{bmatrix} \cdot \mathbf{W}_{1mf} \right) \cdot \mathbf{W}_{2mf} \right) \quad (6)$$

$$d_c = -50 \operatorname{sigm} \left( \operatorname{sigm} \left( \begin{bmatrix} \frac{E}{400} & \frac{\rho}{2600} & \frac{\nu}{0.45} & \frac{\beta}{0.0013} \end{bmatrix} \cdot \mathbf{W}_{1dc} \right) \cdot \mathbf{W}_{2dc} \right) \quad (7)$$

where  $\mathbf{W}_1$  and  $\mathbf{W}_2$  are the weight matrices established and the *sigm* function applied to a matrix corresponds to applying the sigmoid function to each element of the matrix:

$$\operatorname{sigm} \left( \begin{bmatrix} \vdots & & \\ \cdots & a_{ij} & \cdots \\ \vdots & & \end{bmatrix} \right) = \begin{bmatrix} \vdots & & \\ \cdots & \frac{1}{1+e^{-a_{ij}}} & \cdots \\ \vdots & & \end{bmatrix}. \quad (8)$$

The matrices, obtained after complete training and validation, are presented in Figure 5. It is important to note that the cross-damping coefficient  $d_c$  is still assumed to be negative. This assumption accounts for the contributions of wave delay as well as material damping effects.

$$\begin{aligned}
 \mathbf{W}_{1kf} &= \begin{bmatrix} 0.23 & 0.34 & 0.16 & 0.29 & 0.25 & 0.24 & -3.02 & 0.35 & 0.38 & -12.86 & -3.23 & 0.29 & 0.28 & -4.69 & 4.90 & 0.44 & -2.34 & -4.43 & 0.37 & 5.75 \\ -1.91 & -1.09 & -1.95 & -0.45 & -0.29 & -0.47 & -0.65 & -0.79 & -1.39 & 1.15 & -0.55 & -1.84 & -0.40 & 0.55 & -4.18 & -1.70 & -1.15 & -0.19 & -1.74 \\ -1.23 & -1.81 & -1.17 & -1.96 & -1.90 & -1.90 & -1.43 & -1.93 & -1.73 & 0.62 & -1.37 & -1.36 & -1.97 & -0.75 & -8.23 & -1.61 & -1.62 & -0.89 & -2.82 \\ 0.56 & -0.22 & 0.59 & -0.04 & -0.06 & -0.10 & -0.18 & -0.08 & -0.26 & -0.09 & -0.20 & 0.26 & -0.04 & 0.52 & 0.13 & -0.02 & -0.14 & -0.17 & 0.01 \\ -1.16 & -0.52 & 0.35 & -1.75 & 4.37 & 0.72 & 0.16 & -1.17 & -21.35 & -5.85 & -0.63 & -1.64 & -4.43 & 10.20 & -1.38 & -1.80 & -2.34 & -4.43 & 0.37 \\ -0.77 & -0.69 & -0.47 & -3.37 & -1.18 & -0.35 & -0.53 & -0.76 & -2.36 & -0.92 & -0.70 & -0.82 & -0.72 & -7.00 & -0.80 & -0.84 & -1.15 & -0.19 & -1.74 \\ -0.93 & -1.48 & -2.32 & 0.50 & -4.78 & -2.70 & -2.13 & -0.93 & 5.44 & -2.72 & -1.39 & -0.56 & -2.44 & -7.62 & -0.76 & -0.46 & -1.62 & -0.89 & -1.52 \\ 0.28 & -0.02 & -0.26 & -1.51 & 2.20 & -0.30 & -0.22 & 0.32 & -5.43 & 11.28 & 0.03 & 0.52 & 9.83 & -0.36 & 0.39 & 0.60 & -0.14 & -0.17 & 0.01 \\ -0.85 & -0.85 & 3.27 & -0.84 & -0.85 & -0.85 & -19.67 & -0.45 & -0.83 & -0.84 & -0.63 & -1.64 & -4.43 & 10.20 & -1.38 & -1.80 & -2.34 & -4.43 & 0.37 \\ -0.60 & -0.61 & 0.25 & -0.65 & -0.61 & -0.61 & 1.55 & -4.01 & -0.66 & -0.62 & -0.70 & -0.82 & -0.72 & -7.00 & -0.80 & -0.84 & -1.15 & -0.19 & -1.74 \\ -0.12 & -0.12 & -2.54 & -0.10 & -0.12 & -0.12 & 0.70 & 4.13 & -0.10 & -0.11 & -1.39 & -0.56 & -2.44 & -7.62 & -0.76 & -0.46 & -1.62 & -0.89 & -1.52 \\ -0.03 & -0.03 & 0.03 & -0.04 & -0.03 & -0.03 & 0.49 & -0.08 & -0.04 & -0.03 & 0.03 & 0.52 & 9.83 & -0.36 & 0.39 & 0.60 & -0.14 & -0.17 & 0.01 \end{bmatrix} \\
\mathbf{W}_{1df} &= \begin{bmatrix} -1.16 & -0.52 & 0.35 & -1.75 & 4.37 & 0.72 & 0.16 & -1.17 & -21.35 & -5.85 & -0.63 & -1.64 & -4.43 & 10.20 & -1.38 & -1.80 & -2.34 & -4.43 & 0.37 \\ -0.77 & -0.69 & -0.47 & -3.37 & -1.18 & -0.35 & -0.53 & -0.76 & -2.36 & -0.92 & -0.70 & -0.82 & -0.72 & -7.00 & -0.80 & -0.84 & -1.15 & -0.19 & -1.74 \\ -0.93 & -1.48 & -2.32 & 0.50 & -4.78 & -2.70 & -2.13 & -0.93 & 5.44 & -2.72 & -1.39 & -0.56 & -2.44 & -7.62 & -0.76 & -0.46 & -1.62 & -0.89 & -1.52 \\ 0.28 & -0.02 & -0.26 & -1.51 & 2.20 & -0.30 & -0.22 & 0.32 & -5.43 & 11.28 & 0.03 & 0.52 & 9.83 & -0.36 & 0.39 & 0.60 & -0.14 & -0.17 & 0.01 \end{bmatrix} \\
\mathbf{W}_{1kc} &= \begin{bmatrix} -0.85 & -0.85 & 3.27 & -0.84 & -0.85 & -0.85 & -19.67 & -0.45 & -0.83 & -0.84 & -0.63 & -1.64 & -4.43 & 10.20 & -1.38 & -1.80 & -2.34 & -4.43 & 0.37 \\ -0.60 & -0.61 & 0.25 & -0.65 & -0.61 & -0.61 & 1.55 & -4.01 & -0.66 & -0.62 & -0.70 & -0.82 & -0.72 & -7.00 & -0.80 & -0.84 & -1.15 & -0.19 & -1.74 \\ -0.12 & -0.12 & -2.54 & -0.10 & -0.12 & -0.12 & 0.70 & 4.13 & -0.10 & -0.11 & -1.39 & -0.56 & -2.44 & -7.62 & -0.76 & -0.46 & -1.62 & -0.89 & -1.52 \\ -0.03 & -0.03 & 0.03 & -0.04 & -0.03 & -0.03 & 0.49 & -0.08 & -0.04 & -0.03 & 0.03 & 0.52 & 9.83 & -0.36 & 0.39 & 0.60 & -0.14 & -0.17 & 0.01 \end{bmatrix} \\
\mathbf{W}_{1mf} &= \begin{bmatrix} -0.04 & -0.34 & -0.34 & -6.88 & -0.34 & -0.34 & -0.34 & -0.72 & 0.64 & -18.80 & -0.34 & -0.35 & -1.68 & -1.28 & -1.83 & -1.35 & -1.15 & -0.19 & -1.74 \\ -4.83 & -1.97 & -1.97 & -8.06 & -1.97 & -1.97 & 2.94 & -3.01 & 1.26 & -1.97 & -1.97 & -1.51 & -0.17 & -2.62 & -1.95 & -1.99 & -3.30 & -0.51 & -3.30 \\ -0.92 & -0.94 & -0.94 & -15.27 & -0.94 & -0.94 & -0.69 & 0.03 & -3.22 & -0.94 & -0.69 & 0.76 & -1.89 & -0.50 & -1.99 & -1.99 & -3.30 & -0.51 & -3.30 \\ -13.04 & -1.92 & -1.92 & 25.95 & -1.92 & -1.92 & -1.67 & -1.81 & 0.93 & -1.92 & -1.67 & 0.76 & -1.89 & -0.50 & -1.99 & -1.99 & -3.30 & -0.51 & -3.30 \end{bmatrix} \\
\mathbf{W}_{1dc} &= \begin{bmatrix} -3.78 & -0.93 & 2.05 & -0.87 & -1.14 & -4.97 & -6.43 & -1.56 & -7.84 & 1.93 & 0.86 & -0.35 & -1.68 & -1.28 & -1.83 & -1.35 & -1.15 & -0.19 & -1.74 \\ 0.95 & -0.65 & -1.34 & -1.07 & 0.17 & 1.00 & 0.29 & -1.86 & 4.74 & 0.55 & -4.49 & 1.51 & -0.17 & -2.62 & -1.95 & -1.99 & -3.30 & -0.51 & -3.30 \\ 1.25 & -0.40 & -1.24 & -1.04 & 0.97 & 1.69 & -0.14 & -1.98 & 3.18 & -0.77 & 0.76 & -1.89 & -0.50 & -1.99 & -1.99 & -1.99 & -3.30 & -0.51 & -3.30 \\ 5.78 & -2.12 & 2.30 & 1.95 & -2.08 & -1.61 & 0.27 & 0.42 & -6.81 & 4.55 & 1.67 & 3.01 & -1.82 & 0.85 & 0.13 & -0.02 & -0.14 & -0.17 & 0.01 \end{bmatrix} \\
\mathbf{W}_{2kf} &= \begin{bmatrix} -1.64 & -1.53 & -1.63 & -1.44 & -1.42 & -1.44 & 4.37 & 3.17 & -1.49 & -1.59 & -5.95 & 2.59 & -1.62 & -1.44 & 2.52 & 3.79 & -1.64 & 1.51 & 3.35 & -1.62 & 4.63 \end{bmatrix} \\
\mathbf{W}_{2df} &= \begin{bmatrix} -1.51 & -1.47 & -1.44 & 4.37 & 3.17 & -1.49 & -1.59 & -5.95 & 2.59 & -1.62 & -1.44 & 2.52 & 3.79 & -1.64 & 1.51 & 3.35 & -1.62 & 4.63 \end{bmatrix} \\
\mathbf{W}_{2kc} &= \begin{bmatrix} -1.45 & -1.45 & 2.32 & -1.45 & -1.45 & -1.45 & -1.45 & -1.45 & -1.45 & -1.45 & -1.45 & -1.45 & -1.45 & -1.45 & -1.45 & -1.45 & -1.45 & -1.45 & -1.45 & -1.45 & -1.45 \end{bmatrix} \\
\mathbf{W}_{2mf} &= \begin{bmatrix} 44.18 & -3.30 & -3.30 & -0.51 & -3.30 & -3.30 & 2.70 & -2.20 & -2.60 & -3.30 & -3.30 & -3.30 & -3.30 & -3.30 & -3.30 & -3.30 & -3.30 & -3.30 & -3.30 & -3.30 & -3.30 \end{bmatrix} \\
\mathbf{W}_{2dc} &= \begin{bmatrix} -1.83 & -1.35 & -1.95 & 0.78 & 3.18 & -4.59 & 1.62 & -1.99 & 3.54 & -2.12 & -1.99 & -1.65 & 5.73 & -1.83 & -1.35 & -1.95 & 0.78 & 3.18 & -4.59 & 1.62 & -1.99 & 3.54 & -2.12 & -1.99 & -1.65 & 5.73 \end{bmatrix}
\end{aligned}$$

Figure 5. Weight matrices of the trained neural networks (the values of the matrix coefficients have been rounded)



## 4. Results

Several soil configurations were used to validate the CLM model. These data are derived from test cases conducted in the past where manual calibration had been performed. These test soil types were chosen for their relatively possible error on one or more of the CLM model parameters [14]. Table 1 shows an example of results, comparing them to manually obtained data, demonstrating that the implemented neural network is effective and its accuracy is entirely acceptable. These results pertain to a homogeneous soil with the following characteristics: Young modulus  $E = 210$  MPa, density  $\rho = 2000$  kg/m<sup>3</sup>, Poisson ratio  $\nu = 0.35$  and viscous damping coefficient  $\beta = 0.0006$  s. It should be noted that manual calibration cannot be strictly considered a reference, an uncertainty remains on these parameters values as the only criterion used was validation by comparing displacement evolution at a few points under a unit load.

**Table 1.** Example of Comparative Results on the CLM Model

	$k_f$ [MN/m]	$d_f$ [kNs/m]	$k_c$ [MN/m]	$m_f$ [kg]	$d_c$ [kNs/m]
Parameters manually calibrated	54.69	131.65	20.01	171.57	−9.92
Parameters obtained using Eqs. (3)–(7)	47.42	134.27	19.36	191.12	−9.81

To account for layered soils, equivalent homogeneous soils are derived based on the average shear wave velocity  $V_{s,30}$  as defined in Eurocode 8 [17]. This parameter is calculated using the following equation:

$$V_{s,30} = \frac{30 \text{ [m]}}{\sum_i^{n_l} \frac{h_i}{c_{s,i}}} \quad (9)$$

where  $h_i$  is the thickness of the  $i$ -th layer,  $n_l$  is the total number of layers within the top 30 m and  $c_{s,i}$  is the shear wave velocity of the  $i$ -th layer. Thus, equivalent homogeneous soils with  $c_s = V_{s,30}$  are used to model layered soils. The parameter  $V_{s,30}$  represents the mean shear wave velocity in the top 30 m of the soil profile. This simplification yields satisfactory calibration results for soil profiles with smooth stratigraphy.

## 5. Conclusion

To avoid the complexity and burden of a compound model for vehicle/track/soil simulation, a discrete and simplified soil representation, known as the CLM model, has been developed. This model includes coupling through the track contact area and is based on Lysmer's analogue foundation. Coupling spring and damper elements have been incorporated to model the interaction between foundations.

To calibrate the dynamic parameters defined in the model, concise expressions for overall impedances have been established to align with the discrete model parameters. These expressions enable efficient and comprehensive comparisons between discrete and numerical models. A fitting process, based on a neural network, is proposed using these simplified analytical relations, akin to those in Lysmer's analogue model.

The CLM model demonstrates excellent agreement when fitted with numerical results from finite/infinite element soil modelling in various scenarios, including homogeneous soil and layered media. Closed-form solutions are ultimately derived, providing a rapid method for estimating CLM model parameters for typical soil configurations.



## REFERENCES

- 1 Thompson, D. J., Kouroussis, G. and Ntotsios, E. Modelling, simulation and evaluation of ground vibration caused by rail vehicles, *Vehicle System Dynamics*, **57** (7), 936–983, (2019).
- 2 Kouroussis, G., Connolly, D. P. and Verlinden, O. Railway induced ground vibrations — a review of vehicle effects, *International Journal of Rail Transportation*, **2** (2), 69–110, (2014).
- 3 Connolly, D. P., Kouroussis, G., Laghrouche, O., Ho, C. and Forde, M. C. Benchmarking railway vibrations — track, vehicle, ground and building effects, *Construction and Building Materials*, **92**, 64–81, (2015).
- 4 Rücker, W. Dynamic interaction of a railroad-bed with the subsoil, *Soil Dynamics & Earthquake Engineering Conference*, Southampton (England), vol. 2, pp. 435–448, (1982).
- 5 Knothe, K. and Wu, Y. Receptance behaviour of railway track and subgrade, *Archive of Applied Mechanics*, **68**, 457–470, (1998).
- 6 Gazetas, G. Analysis of machine foundation vibrations: state of the art, *Soil Dynamics and Earthquake Engineering*, **2** (1), 2–42, (1983).
- 7 Ju, S. H. Evaluating foundation mass, damping and stiffness by the least-squares method, *Earthquake Engineering & Structural Dynamics*, **32** (9), 1431–1442, (2003).
- 8 Olivier, B., Verlinden, O. and Kouroussis, G. A vehicle/track/soil model using co-simulation between multi-body dynamics and finite element analysis, *International Journal of Rail Transportation*, **8** (2), 135–158, (2020).
- 9 Olivier, B., Verlinden, O. and Kouroussis, G. Comparison of X–T and X–X co-simulation techniques applied on railway dynamics, *Multibody System Dynamics*, **55** (1-2), 39–56, (2022).
- 10 Connolly, D. P., Kouroussis, G., Giannopoulos, A., Verlinden, O., Woodward, P. K. and Forde, M. C. Assessment of railway vibrations using an efficient scoping model, *Soil Dynamics and Earthquake Engineering*, **58**, 37–47, (2014).
- 11 Connolly, D. P., Kouroussis, G., Woodward, P. K., Verlinden, O., Giannopoulos, A. and Forde, M. C. Scoping prediction of re-radiated ground-borne noise and vibration near high speed rail lines with variable soils, *Soil Dynamics and Earthquake Engineering*, **66**, 78–88, (2014).
- 12 López-Mendoza, D., Connolly, D. P., Romero, A., Kouroussis, G. and Galvín, P. A transfer function method to predict building vibration and its application to railway defects, *Construction and Building Materials*, **232**, 117217, (2020).
- 13 López-Mendoza, D., Romero, A., Connolly, D. and Galvín, P. Scoping assessment of building vibration induced by railway traffic, *Soil Dynamics and Earthquake Engineering*, **93**, 147–161, (2017).
- 14 Kouroussis, G., Gazetas, G., Anastasopoulos, I., Conti, C. and Verlinden, O. Discrete modelling of vertical track–soil coupling for vehicle–track dynamics, *Soil Dynamics and Earthquake Engineering*, **31** (12), 1711–1723, (2011).
- 15 Kouroussis, G., Anastasopoulos, I., Gazetas, G., Conti, C. and Verlinden, O. Effect of the track/soil coupling on the railway-induced ground vibrations, *19th International Congress on Sound and Vibration (ICSV19)*, Vilnius (Lithuania), (2012).
- 16 Aggarwal, C. C., *Neural Networks and Deep Learning*, Springer Cham (2023).
- 17 European Committee for Standardization, (2004), *Eurocode 8: Design of structures for earthquake resistance — Part 1: General rules, seismic actions and rules for buildings*.